K$_3$[Tb$_x$Eu$_{1-x}$Ge$_3$O$_8$(OH)$_2$] (x = 1, 0.88, 0.67, 0): 2D-Layered Lanthanide Germanates with Tunable Photoluminescent Properties

Xi Wang,[†] Yu Wang,[†] Qiong Liu,[‡] Yi Li,[†] Jihong Yu,*[,†] and Ruren Xu[†]

[†]State Key Laboratory of Inorganic Synthesis and Preparative Chemistry, College of Chemistry, Jilin University, Changchun 130012, People's Republic of China

[‡]Changchun Institute of Applied Chemistry, Chinese Academy of Sciences, Changchun 130022, People's Republic of China

Ⓢ Supporting Information

ABSTRACT: A family of novel 2D-layered lanthanide germanates K$_3$[Tb$_x$Eu$_{1-x}$Ge$_3$O$_8$(OH)$_2$] (x = 1, 0.88, 0.67, 0; denoted as TbGeO-JU-87, Tb$_{0.88}$Eu$_{0.12}$GeO-JU-87, Tb$_{0.67}$Eu$_{0.33}$GeO-JU-87, and EuGeO-JU-87) were synthesized under mild hydrothermal conditions in a concentrated gel system. They are isostructural, as confirmed by the powder X-ray diffraction analysis. The single-crystal X-ray diffraction analysis of EuGeO-JU-87 reveals that it is a 2D-layered [EuGe$_3$O$_8$(OH)$_2$]$_n^{3n-}$ anionic framework, which is built up from GeO$_4$H/GeO$_4$ tetrahedra and EuO$_6$ octahedra by sharing vertex O atoms. Charge neutrality is achieved by K$^+$ ions located in the free void space. Interestingly, photoluminescence studies show that Tb$_{0.88}$Eu$_{0.12}$GeO-JU-87 and Tb$_{0.67}$Eu$_{0.33}$GeO-JU-87 exhibit a high Tb^{3+}-to-Eu^{3+} energy-transfer efficiency and the Tb$_x$Eu$_{1-x}$GeO-JU-87 system displays tunable photoluminescent properties.
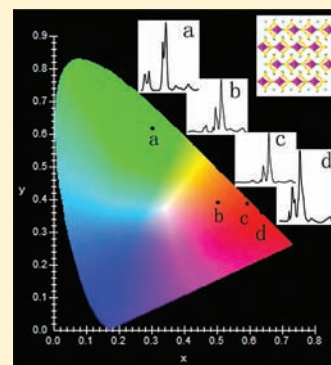
INTRODUCTION

The microporous lanthanide silicates exhibit a rich structural chemistry and display potential applications in fast alkali-ion conductors and optical materials.[1] Many lanthanide silicates that are built from SiO$_4$ tetrahedra and LnO$_n$ (n ≥ 6) polyhedra have been successfully prepared by using mild hydrothermal,[2] flux-growth,[3] and high-temperature/high-pressure hydrothermal[4] methods in the past decades. Notably, some structures are versatile, which allows the introduction of a couple of Ln^{3+} ions into the frameworks.[2f−j,5−10] Importantly, it is possible to fine-tune their photoluminescent properties by changing the excitation wavelengths and/or the compositions due to the energy transfer between the Ln^{3+} pairs (e.g., Tb^{3+}/Eu^{3+}, Ce^{3+}/Tb^{3+}, Gd^{3+}/Tb^{3+}). For instance, the chromaticity of the Ce$_{1-(a+b)}$Tb$_a$Eu$_b$-AV-20 system[6] was tunable by varying the Ce/Tb/Eu ratios, and a full-color phosphor Ce$_{0.53}$Tb$_{0.35}$Eu$_{0.12}$-AV-20 can be obtained. In summary, a lot of research has been focused on the exploration of interesting structures and the luminescent properties of lanthanide silicates. However, much less work has been reported on the lanthanide germanates.[11−15] In contrast to the microporous lanthanide silicates mentioned above, most lanthanide germanates are dense phases that are comprised of anionic groups (e.g., [GeO$_4$]$^{4-}$,[11] [GeO$_5$]$^{6-}$,[12] [Ge$_2$O$_6$]$^{4-}$,[13] and [Ge$_2$O$_7$]$^{6-}$[14]) that are further connected via LnO$_n$ (n ≥ 6) polyhedra. Their synthesis methods are mainly limited to the flux-growth and high-temperature/high-pressure hydrothermal methods. Recently, our group has synthesized a high-pressure-stable photoluminescent europium germanate NaEu$_3$(GeO$_4$)$_2$(OH)$_2$ using a mild hydrothermal synthesis method (230 °C).[11b] However, synthesizing open-framework lanthanide germanates under mild hydrothermal conditions is still a challenge.

Here, we report a family of novel 2D-layered compounds K$_3$[Tb$_x$Eu$_{1-x}$Ge$_3$O$_8$(OH)$_2$] (x = 1, 0.88, 0.67, 0; denoted as TbGeO-JU-87, Tb$_{0.88}$Eu$_{0.12}$GeO-JU-87, Tb$_{0.67}$Eu$_{0.33}$GeO-JU-87, and EuGeO-JU-87), which are synthesized by using a mild hydrothermal synthesis method at 200 °C. They are structurally analogous to some lanthanide silicates K$_3$LnSi$_3$O$_8$(OH)$_2$ (Ln = Y^{3+}, Eu^{3+}, Tb^{3+}, Er^{3+}; denoted as AV-22).[2g] The energy transfer from Tb^{3+} to Eu^{3+} in Tb$_{0.88}$Eu$_{0.12}$GeO-JU-87 and Tb$_{0.67}$Eu$_{0.33}$GeO-JU-87 has been studied. Interestingly, their emission colors shift to different regions in the CIE chromaticity diagram because of the different Tb^{3+}/Eu^{3+} contents, revealing tunable photoluminescence.

EXPERIMENTAL SECTION

Synthesis. In typical syntheses of EuGeO-JU-87 and TbGeO-JU-87, the gel was made by mixing potassium hydroxide (0.28 g), germanium dioxide (0.15 g), boric acid (0.05 g), europium nitrate hexahydrate (0.088 g) or terbium nitrate hexahydrate (0.090 g), and 0.1 mL of deionized water. The mixture with a molar composition of 3.5:1.0:0.56:0.07 KOH/GeO$_2$/H$_3$BO$_3$/Eu$_2$O$_3$ or 0.035:4.72 Tb$_4$O$_7$/H$_2$O was heated in a Teflon-lined stainless steel autoclave (15 mL) at 200 °C for 7 days under static conditions in an oven. The resulting colorless crystals were filtered, washed with deionized water, and dried at 353 K. The Tb^{3+}/Eu^{3+} mixed samples were prepared by introducing the desired Tb^{3+} and Eu^{3+} contents in the initial gel.

Characterizations. Powder X-ray diffraction (XRD) data were collected on a Rigaku D/Max 2550 X-ray diffractometer using Cu Kα

radiation (λ = 1.5418 Å). Inductively coupled plasma (ICP) analysis was performed on a Perkin-Elmer Optima 3300 DV ICP spectrometer. Energy-dispersive spectroscopy (EDS) analysis was carried out using an EDS System with a window attached to a JEOL JSM-6700F scanning electron microscope. IR spectra were recorded on a Nicolet Impact 410 FT-IR spectrometer using the KBr pellet technique. The excitation and emission spectra of the samples were detected by a Fluoromax-4 spectrofluorometer (Horiba). The emission spectra were corrected for detection and optical spectral response of the spectrofluorometer. The excitation spectra were corrected for spectral distribution of the lamp intensity using a photodiode reference detector. Luminescent decay curves were recorded by an oscillograph (Tektronix, TDS3052, 500 MHz, 5 Gs s^{-1}), with a 355-nm light excitation source.

Single-Crystal Structure Determination. The suitable single crystal with dimensions of 0.15 × 0.12 × 0.08 mm for EuGeO-JU-87 was selected for single-crystal XRD analysis. Structural analysis was performed on a Bruker AXS SMART APEX II diffractometer using graphite-monochromated Mo Kα radiation (λ = 0.71073 Å) at a temperature of 296 ± 2 K. Data processing was accomplished with the *SAINT* processing program. The structure was solved by direct methods and refined by full-matrix least-squares techniques with the *SHELXTL* crystallographic software package. All of the K, Eu, Ge, and O atoms were unambiguously located in the Fourier maps. The H atoms attached to the GeO$_4$ tetrahedron were placed geometrically. A summary of the crystallographic data is presented in Table 1. The selected bond lengths [Å] and angles [deg] for EuGeO-JU-87 are presented in Table S1 (Supporting Information).

Table 1. Crystal Data and Structure Refinement for EuGeO-JU-87

identification code	EuGeO-JU-87
empirical formula	HEu$_{0.5}$Ge$_{1.5}$K$_{1.5}$O$_5$
fw	324.52
temperature (K)	296(2)
wavelength (Å)	0.71073
cryst syst, space group	orthorhombic, *Pnma*
unit cell dimens	a = 13.7053(7) Å, α = 90°
	b = 13.7236(7) Å, β = 90°
	c = 6.1051(3) Å, γ = 90°
volume (Å^3)	1148.28(10)
Z, calcd density (mg m^{-3})	8, 3.754
abs coeff (mm^{-1})	14.288
F(000)	1192
cryst size (mm^3)	0.15 × 0.12 × 0.08
θ range for data collection	2.97–28.35°
limiting indices	−18 ≤ h ≤ 10, −16 ≤ k ≤ 18, −8 ≤ l ≤ 7
reflns collected/unique	7894/1491 [R(int) = 0.0391]
completeness to θ = 28.13° (%)	99.9
abs corrn	semiempirical from equivalents
max and min transmn	0.4311 and 0.2041
refinement method	full-matrix least squares on F^2
data/restraints/param	1491/0/86
GOF on F^2	1.041
final R indices [I > 2σ(I)]	R1 = 0.0250, wR2 = 0.0551
R indices (all data)	R1 = 0.0325, wR2 = 0.0583
largest diff peak and hole (e Å^{-3})	2.943 and −1.036

■ RESULTS AND DISCUSSION

Synthesis and Characterizations. Different from the lanthanide silicates hydrothermally prepared by using an excess amount of water as the solvent, these germanates were synthesized in a concentrated gel system with a low H$_2$O/

GeO$_2$ molar ratio. Only the amorphous phase was obtained with an increase of the H$_2$O/GeO$_2$ molar ratio. Notice that EuGeO-JU-87 could also be obtained in the absence of boric acid in the synthesis gel. The addition of boric acid favored the formation of single crystals of EuGeO-JU-87 with good quality and a high yield.

Figure 1 shows the powder XRD patterns of the four as-synthesized compounds, which are consistent with the
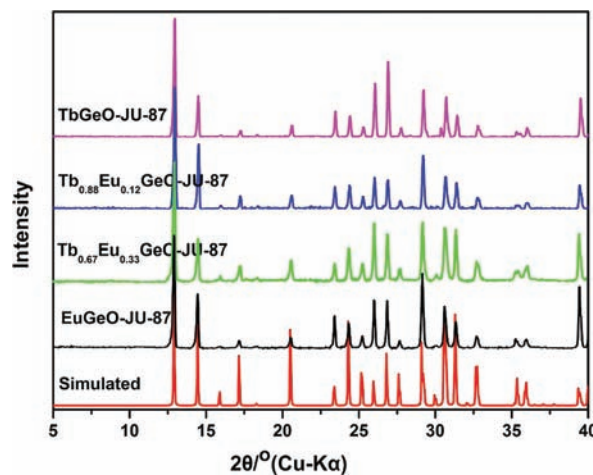
Figure 1. Simulated powder XRD pattern of EuGeO-JU-87 and experimental XRD patterns of EuGeO-JU-87, Tb$_{0.88}$Eu$_{0.12}$GeO-JU-87, Tb$_{0.67}$Eu$_{0.33}$GeO-JU-87, and TbGeO-JU-87.

simulated one on the basis of single-crystal structural analysis of EuGeO-JU-87, indicating that they are isostructural. The difference of the intensity of some reflections in the experimental XRD patterns from those observed in the simulated pattern might result from preferential orientation related to the sheet morphology of the crystals. Table S2 in the Supporting Information displays the ICP and EDS analysis results of the four compounds (EuGeO-JU-87, TbGeO-JU-87, Tb$_{0.88}$Eu$_{0.12}$GeO-JU-87, and Tb$_{0.67}$Eu$_{0.33}$GeO-JU-87), which are in agreement with the theoretically calculated values. No boron content was detected by either ICP or EDS analysis for samples synthesized in the presence of boric acid in the synthesis gel. In addition, the relative molar ratio of Tb/Eu (0.88/0.12 and 0.67/0.33) in Tb$_{0.88}$Eu$_{0.12}$GeO-JU-87 and Tb$_{0.67}$Eu$_{0.33}$GeO-JU-87 is consistent with that in the synthesis gel, respectively.

Crystal Structure of EuGeO-JU-87. The structure of EuGeO-JU-87 was determined by single-crystal structural analysis, and its structure is analogous to some lanthanide silicates K$_3$LnSi$_3$O$_8$(OH)$_2$ (Ln = Y^{3+}, Eu^{3+}, Tb^{3+}, Er^{3+}; denoted as AV-22).[2g] EuGeO-JU-87 crystallizes in the *Pnma* space group (No. 62) with a = 13.7053(7) Å, b = 13.7236(7) Å, and c = 6.1051(3) Å. Each asymmetric unit contains one crystallographically distinct Eu atom, two distinct Ge atoms, and two distinct K ions (Figure S1 in the Supporting Information). The Eu atom is six-coordinated to O atoms to form a EuO$_6$ octahedron. Ge(1) is connected to three O atoms and a hydroxyl OH to form a Ge(1)O$_4$H tetrahedron, while Ge(2) is coordinated to four O atoms to form a Ge(2)O$_4$ tetrahedron. The existence of Ge−O bonds and an −OH group is confirmed by IR analysis (Figure S2 in the Supporting Information). The peaks at 810, 781, and 760 cm^{-1} can be assigned to the asymmetric stretching vibrations of the Ge−O bonds, and the bands at about 3000 cm^{-1} correspond to the −OH groups.[16]

K(1) and K(2) ions are surrounded by 8 and 11 O atoms [K(1)−O, 2.703(4)−3.356(2) Å; K(2)−O, 2.688(5)−3.293(4) Å], respectively. EuGeO-JU-87 is built up from GeO_4H/GeO_4 tetrahedra and EuO_6 octahedra by sharing vertex O atoms, giving rise to a 2D-layered $[EuGe_3O_8(OH)_2]_n^{3n-}$ anionic framework. Figure 2a shows the layer viewed along the [010]

Figure 2. (a) Single layer with three and seven rings viewed along the [010] direction. (b) Polyhedral view of EuGeO-JU-87 along the [001] direction. Color code: Eu, purple; Ge, yellow; K, green; O, red; H, blue.

direction, which contains three and seven rings. The seven-ring window is delimited by two GeO_4H and two GeO_4 tetrahedra and three EuO_6 octahedra. Figure 2b shows the 2D layers viewed along the [001] direction, which are stacked in the sequence of [ABAB...]. The layers are interconnected through the O−H···O hydrogen bonds [O(6)−H(1), 0.820 Å; H(1)···O(3), 1.860 Å; O(6)···O(3), 2.676 Å] between the neighboring Ge−OH groups. The K^+ ions are located in the free void space to achieve the charge balance. $K^+(1)$ ions are arranged in the interlayer space, while $K^+(2)$ ions are located in the seven-ring windows.

Photoluminescence Study. Figure 3a shows the room temperature (RT) emission spectra of the four compounds. The emission spectrum of EuGeO-JU-87 excited at 394 nm displays a series of sharp lines from 550 to 720 nm, which are assigned to the $^5D_0 \rightarrow {}^7F_{0-4}$ transitions. The intensity of the $^5D_0 \rightarrow {}^7F_2$ electric-dipole transition is stronger than that of the $^5D_0 \rightarrow {}^7F_1$ magnetic-dipole transition. This indicates that there
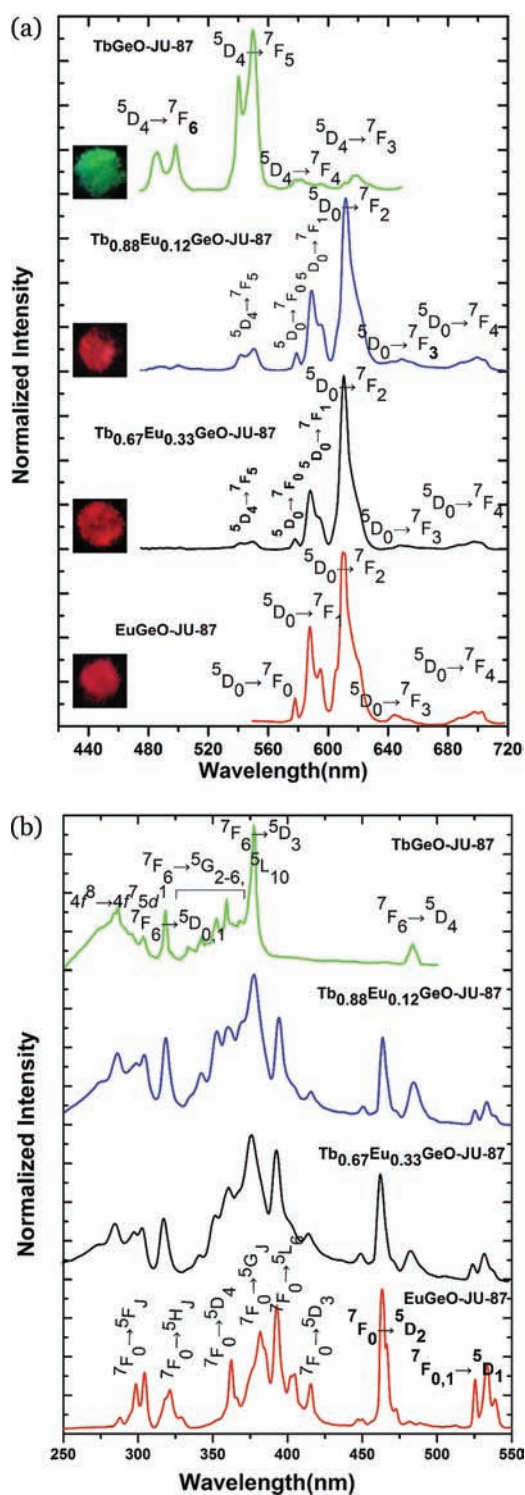
Figure 3. (a) RT emission spectra of TbGeO-JU-87 (λ_{ex} = 377 nm), $Tb_{0.88}Eu_{0.12}$GeO-JU-87 (λ_{ex} = 377 nm), $Tb_{0.67}Eu_{0.33}$GeO-JU-87 (λ_{ex} = 377 nm), and EuGeO-JU-87 (λ_{ex} = 394 nm). The photographs are taken under UV light illumination (365 nm). (b) RT excitation spectra of TbGeO-JU-87 (λ_{em} = 540 nm), $Tb_{0.88}Eu_{0.12}$GeO-JU-87 (λ_{em} = 613 nm), $Tb_{0.67}Eu_{0.33}$GeO-JU-87 (λ_{em} = 613 nm), and EuGeO-JU-87 (λ_{em} = 613 nm).

is a lack of an inversion-symmetry center on Eu^{3+} ions, which is consistent with the asymmetric Eu^{3+} location according to structural analysis. For TbGeO-JU-87, the emission spectrum excited at 377 nm exhibits several sharp lines between 475 and

675 nm, which are associated with the $^5D_4 \rightarrow {}^7F_J$ ($J = 3-6$) transitions of Tb^{3+} with the strongest at about 540 and 552 nm ($^5D_4 \rightarrow {}^7F_5$). The luminescence from the higher (e.g., $^5D_3$) excited states was not detected, indicating the efficient nonradiative relaxation to the $^5D_4$ level. For $Tb_{0.88}Eu_{0.12}GeO$-JU-87 and $Tb_{0.67}Eu_{0.33}GeO$-JU-87, their emission spectra excited in the Tb^{3+} (377 nm) levels show both typical Eu^{3+} and Tb^{3+} lines with the strongest $^5D_0 \rightarrow {}^7F_2$ transitions, implying the occurrence of Tb^{3+}-to-Eu^{3+} energy transfer.[2f,g,8−10] Figure 3b shows the RT excitation spectra of the four compounds. The excitation spectrum of EuGeO-JU-87 from 250 to 550 nm emitted at 613 nm shows a series of sharp lines with the stronger lines, namely, $^7F_0 \rightarrow {}^5D_2$. In the excitation spectrum of TbGeO-JU-87 emitted at 540 nm, the broad band between 250 and 280 nm is ascribed to the spin-forbidden (high-spin) interconfigurational $4f^8 \rightarrow 4f^75d^1$ transition. The clearly observed sharp lines from 300 to 500 nm are associated with $^7F_6 \rightarrow {}^5D_{0,1}$, $^7F_6 \rightarrow {}^5G_{2-6}$,$^5 L_{10}$, and $^7F_6 \rightarrow {}^5D_{3,4}$ transitions. The excitation spectra monitored at the main $^5D_0 \rightarrow {}^7F_2$ line (613 nm) of Eu^{3+} for $Tb_{0.88}Eu_{0.12}GeO$-JU-87 and $Tb_{0.67}Eu_{0.33}GeO$-JU-87 display both characteristic Eu^{3+} and Tb^{3+} lines, which also reveals the existence of Tb^{3+}-to-Eu^{3+} energy transfer.[2f,g,8−10]

The RT fluorescence decay curve of the $^5D_0 \rightarrow {}^7F_2$ transitions (613 nm) for EuGeO-JU-87 (Figure 4a) is well-fitted by an exponential function, yielding the lifetime value of $t = 0.84$ ms, which suggests that there is only one Eu^{3+} environment. This is in agreement with the presence of one crystallographically distinct Eu^{3+} according to its structural analysis. For TbGeO-JU-87, Figure 4a also shows the decay curve of the $^5D_4 \rightarrow {}^7F_5$ transitions (540 nm), which is well-fitted by an exponential function, yielding a lifetime value of $t = 1.02$ ms. It also confirms the presence of one Tb^{3+} environment.

To further study the energy transfer in $Tb_{0.88}Eu_{0.12}GeO$-JU-87 and $Tb_{0.67}Eu_{0.33}GeO$-JU-87, both the Eu^{3+} and Tb^{3+} decay curves are investigated. Notably, the clearly observed rising step of the Eu^{3+} curve detected at the $^5D_0 \rightarrow {}^7F_2$ transitions (613 nm) is evidence for the grow-in behavior of Eu^{3+} ions (Figure 4b and inset). That is, the energy transfer results in the corresponding changes in the populations of related donor and acceptor energy levels, which further leads to changes in the Eu^{3+} fluorescence intensity. As can be seen in Figure 4b, the intensity increases with increasing time, reaching a maximum, and decreases until the decay process completes. Their Eu^{3+} decay curves (not in the natural log scale) can be well-fitted by biexponential function $I(t) = A_1 \exp(-t/\tau_1) + A_2 \exp(-t/\tau_2)$, where $I(t)$ is the luminescence intensity, τ_1 is a decay time, τ_2 is a decay or rise time, and A_1 and A_2 present the relative contributions of the components with τ_1 and τ_2 lifetimes, respectively. As shown in Table 2, the A_2 values are negative for both $Tb_{0.88}Eu_{0.12}GeO$-JU-87 and $Tb_{0.67}Eu_{0.33}GeO$-JU-87, indicating that τ_2 is a rise time,[17] which further confirms the existence of energy transfer in the two compounds. Notice that the rise and decay times related to the fitted function are the average times. Moreover, the rise time decreases with increasing Eu^{3+} concentration, which implies that the rate of Tb^{3+}-to-Eu^{3+} energy transfer is dependent on the Eu^{3+} concentration.[9] Figure 4a also shows the Tb^{3+} decay curves detected at $^5D_4 \rightarrow {}^7F_5$ transitions (540 nm) of $Tb_{0.88}Eu_{0.12}GeO$-JU-87 and $Tb_{0.67}Eu_{0.33}GeO$-JU-87, which are well-fitted by an exponential function, yielding lifetime values of $t = 0.18$ and 0.07 ms, respectively. The values are significantly reduced compared
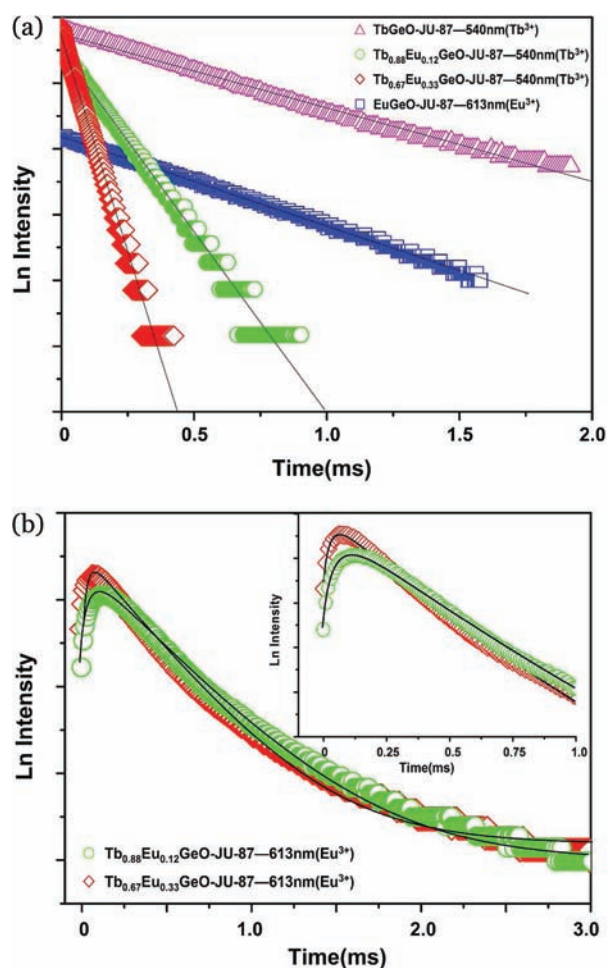
Figure 4. (a) RT fluorescence decay curves (in a natural log scale) detected at 613 nm (Eu^{3+}) for EuGeO-JU-87 and detected at 540 nm (Tb^{3+}) for TbGeO-JU-87, $Tb_{0.88}Eu_{0.12}GeO$-JU-87, and $Tb_{0.67}Eu_{0.33}GeO$-JU-87. (b) RT fluorescence decay curves (in a natural log scale) detected at 613 nm for $Tb_{0.88}Eu_{0.12}GeO$-JU-87 and $Tb_{0.67}Eu_{0.33}GeO$-JU-87. Inset: Decay process within 1 ms. The solid line represents the best fit to the data. All of the samples are excited at 355 nm.

Table 2. Parameters Calculated from the Fit of the Equation[a]

sample	A_1	τ_1 (μs)	A_2	τ_2 (μs)
$Tb_{0.88}Eu_{0.12}GeO$-JU-87	1.4160	494.1	−1.0017	56.7
$Tb_{0.67}Eu_{0.33}GeO$-JU-87	1.5741	486.0	−0.9191	28.7

[a]$I(t) = A_1 \exp(-t/\tau_1) + A_2 \exp(-t/\tau_2)$.

with TbGeO-JU-87 ($t = 1.02$ ms) because of the contribution of Tb^{3+} as a donor in energy transfer.[2g] The energy-transfer efficiency could be calculated by $E = 1 - t/\tau_0$,[2g,8] where τ_0 and t are the Tb^{3+} lifetimes in the absence and presence of Eu^{3+}, respectively. The energy-transfer efficiency of $Tb_{0.67}Eu_{0.33}GeO$-JU-87(0.93) is higher than that of $Tb_{0.88}Eu_{0.12}GeO$-JU-87 (0.82). This reveals that an increase of the concentration of acceptors appropriately might increase the energy-transfer efficiency.

Figure 5 shows the x and y emission color coordinates of the four compounds in the 1931 CIE chromaticity diagram. Their emission colors shift closer to the red region with increasing
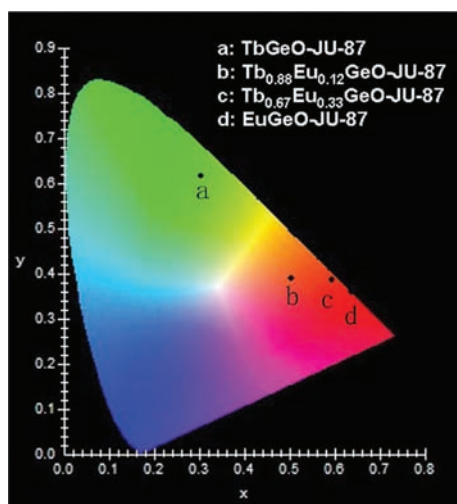
Figure 5. x and y emission color coordinates in the 1931 CIE chromaticity diagram for TbGeO-JU-87 ($x = 0.3047$, $y = 0.6196$; $\lambda_{ex} = 377$ nm), $Tb_{0.88}Eu_{0.12}GeO$-JU-87 ($x = 0.5037$, $y = 0.3928$; $\lambda_{ex} = 377$ nm), $Tb_{0.67}Eu_{0.33}GeO$-JU-87 ($x = 0.5956$, $y = 0.3874$; $\lambda_{ex} = 377$ nm), and EuGeO-JU-87 ($x = 0.6372$, $y = 0.3624$; $\lambda_{ex} = 394$ nm).

Eu^{3+} concentration, which indicates that their luminescent properties can be tunable by different Tb^{3+}/Eu^{3+} ratios.

CONCLUSIONS

Four isostructural 2D-layered lanthanide germanates $K_3[Tb_xEu_{1-x}Ge_3O_8(OH)_2]$ ($x = 1$, 0.88, 0.67, 0) have been hydrothermally synthesized in a concentrated gel system at 200 °C. EuGeO-JU-87 is a 2D-layered framework with the [ABAB...] stacking sequence of $[EuGe_3O_8(OH)_2]_n^{3n-}$ anionic layers. $Tb_{0.67}Eu_{0.33}GeO$-JU-87 has a higher Tb^{3+}-to-Eu^{3+} energy-transfer efficiency than $Tb_{0.88}Eu_{0.12}GeO$-JU-87. Their optical properties are tunable, and the emission color shifts closer to the red region with increasing Eu^{3+} concentration. The successful mild hydrothermal synthesis of Tb^{3+}/Eu^{3+} mixed germanates and the discovery of their tunable photoluminescent properties will provide a feasible route to preparing many more novel fine-tuned optical lanthanide germanates.

ASSOCIATED CONTENT

Ⓢ Supporting Information

Thermal ellipsoid plot (50% probability) and atomic labeling scheme of EuGeO-JU-87, IR spectra of EuGeO-JU-87, TbGeO-JU-87, $Tb_{0.88}Eu_{0.12}GeO$-JU-87, and $Tb_{0.67}Eu_{0.33}GeO$-JU-87, selected bond lengths [Å] and angles [deg] for EuGeO-JU-87, ICP and EDS analysis data of EuGeO-JU-87, TbGeO-JU-87, $Tb_{0.88}Eu_{0.12}GeO$-JU-87, and $Tb_{0.67}Eu_{0.33}GeO$-JU-87, and X-ray crystallographic file (CIF) of EuGeO-JU-87. This material is available free of charge via the Internet at http://pubs.acs.org.

AUTHOR INFORMATION

Corresponding Author

*E-mail: jihong@jlu.edu.cn.

Notes

The authors declare no competing financial interest.

ACKNOWLEDGMENTS

REFERENCES

(1) Rocha, J.; Carlos, L. D. *Curr. Opin. Solid State Mater. Sci.* **2003**, 7, 199.

(2) (a) Rocha, J.; Ferreira, P.; Lin, Z.; Brandaõ, P.; Ferreira, A.; Pedrosa de Jesus, J. D. *Chem. Commun.* **1997**, 2103. (b) Rocha, J.; Ferreira, P.; Lin, Z.; Brandaõ, P.; Ferreira, A.; Pedrosa de Jesus, J. D. *J. Phys. Chem. B* **1998**, 102, 4739. (c) Rocha, J.; Ferreira, P.; Carlos, L. D.; Ferreira, A. *Angew. Chem., Int. Ed.* **2000**, 39, 3276. (d) Ananias, D.; Ferreira, A.; Rocha, J.; Ferreira, P.; Rainho, J. P.; Morais, C.; Carlos, L. D. *J. Am. Chem. Soc.* **2001**, 123, 5735. (e) Jeong, H. K.; Chandrasekaran, A.; Tsapatsis, M. *Chem. Commun.* **2002**, 2398. (f) Ferreira, A.; Ananias, D.; Carlos, L. D.; Morais, C. M.; Rocha, J. *J. Am. Chem. Soc.* **2003**, 125, 14573. (g) Ananias, D.; Kostova, M.; Almeida Paz, F. A.; Ferreira, A.; Carlos, L. D.; Klinowski, J.; Rocha, J. *J. Am. Chem. Soc.* **2004**, 126, 10410. (h) Ananias, D.; Ferdov, S.; Almeida Paz, F. A.; Sá Ferreira, R. A.; Ferreira, A.; Geraldes, C. F. G. C.; Carlos, L. D.; Lin, Z.; Rocha, J. *Chem. Mater.* **2008**, 20, 205. (i) Ananias, D.; Kostova, M.; Paz, F. A. A.; Neto, A. N. C.; De Moura, R. T., Jr.; Malta, O. L.; Carlos, L. D.; Rocha, J. *J. Am. Chem. Soc.* **2009**, 131, 8620. (j) Ananias, D.; Almeida Paz, F. A.; Carlos, L. D.; Geraldes, C. F. G. C.; Rocha, J. *Angew. Chem., Int. Ed.* **2006**, 45, 7938. (k) Wang, G.; Li, J.; Yu, J.; Chen, P.; Pan, Q.; Song, H.; Xu, R. *Chem. Mater.* **2006**, 18, 5637. (l) Wang, G.; Yan, W.; Chen, P.; Wang, X.; Qian, K.; Su, T.; Yu, J. *Microporous Mesoporous Mater.* **2007**, 105, 58. (m) Wang, X.; Li, J.; Wang, G.; Han, Y.; Su, T.; Li, Y.; Yu, J.; Xu, R. *Solid State Sci.* **2010**, 12, 422. (n) Cadoni, M.; Cheah, Y. L.; Ferraris, G. *Acta Crystallogr., Sect. B: Struct. Sci.* **2010**, 66, 158. (o) Wang, X.; Li, J.; Han, Y.; Li, Y.; Yu, J.; Xu, R. *Chem. Mater.* **2011**, 23, 2842.

(3) (a) Chiang, P. Y.; Lin, T. W.; Dai, J. H.; Chang, B. C.; Lii, K. H. *Inorg. Chem.* **2007**, 46, 3619. (b) Tang, M. F.; Chiang, P. Y.; Su, Y. H.; Jung, Y. C.; Hou, G. Y.; Chang, B. C.; Lii, K. H. *Inorg. Chem.* **2008**, 47, 8985.

(4) (a) Huang, M. Y.; Chen, Y. H.; Chang, B. C.; Lii, K. H. *Chem. Mater.* **2005**, 17, 5743. (b) Zhao, X.; Li, J.; Chen, P.; Li, Y.; Chu, Q.; Liu, X.; Yu, J.; Xu, R. *Inorg. Chem.* **2010**, 49, 9833.

(5) Ananias, D.; Ferreira, A.; Carlos, L. D.; Rocha, J. *Adv. Mater.* **2003**, 12, 980.

(6) Evans, R. C.; Carlos, L. D.; Douglas, P.; Rocha, J. *J. Mater. Chem.* **2008**, 18, 1100.

(7) Kostova, M. H.; Sá Ferreira, R. A.; Ananias, D.; Carlos, L. D.; Rocha, J. *J. Phys. Chem. B* **2006**, 110, 15312.

(8) Kowalchuk, C. M.; Paz, F. A. A.; Ananias, D.; Pattison, P.; Carlos, L. D.; Rocha, J. *Chem.—Eur. J.* **2008**, 14, 8157.

(9) Evans, R. C.; Ananias, D.; Douglas, A.; Douglas, P.; Carlos, L. D.; Rocha, J. *J. Phys. Chem. C* **2008**, 112, 260.

(10) Moreira dos Santos, A.; Marques, F. M. B.; Carlos, L. D.; Rocha, J. *J. Mater. Chem.* **2006**, 16, 3139.

(11) (a) Kharakh, E. A.; Chichagov, A. V.; Belov, N. V. *Kristallografiya* **1910**, 15, 1064. (b) Zhao, X.; Yan, T.; Wang, K.; Yan, Y.; Zou, B.; Yu, J.; Xu, R. *Eur. J. Inorg. Chem.* **2012**, DOI: 10.1002/ejic.201200200

(12) Kato, K.; Sekita, M.; Kimura, S. *Acta Crystallogr., Sect. B* **1979**, 35, 2201.

(13) Chen, P. L.; Chiang, P. Y.; Yeh, H. C.; Chang, B. C.; Lii, K. H. *Dalton Trans.* **2008**, 13, 1721.

(14) Chiragov, M. I.; Mamedo, Kh. S.; Kulieva, T. Z. *Kristallografiya* **1983**, 28, 1035.

(15) Zhang, J. H.; Li, P. X.; Mao, J. G. *Dalton Trans.* **2010**, 39, 5301.

(16) Beitone, L.; Loiseau, T.; Férey, G. *Inorg. Chem.* **2002**, 41, 3962.

(17) (a) Zhang, X.; Zhang, J.; Liang, L.; Su, Q. *Mater. Res. Bull.* **2005**, 40, 281. (b) Zhang, X.; Lang, H.; Seo, H. J. *J. Fluoresc.* **2011**, 21, 1111.